Lecture 3: CMB Physics, Acoustic Oscillations, and Large-Scale Structure

Graduate Course in Astroparticles and Cosmology

Luca Visinelli

Università di Salerno, Spring 2026

Plan of the lecture

1. The CMB as a probe of primordial perturbations
2. Linear perturbations and primordial spectra
3. From primordial perturbations to CMB anisotropies
4. Photon–baryon acoustic oscillations
5. Growth of large-scale structure
6. Matter power spectrum and transfer function
7. Baryon acoustic oscillations
8. Synthesis

The Cosmic Microwave Background

The Cosmic Microwave Background is the radiation released when the Universe became transparent at recombination. It provides a direct image of the photon–baryon plasma at the surface of last scattering.

The observed temperature field is written as

$$T(\hat{\mathbf{n}}) = \bar{T}\left[1 + \Theta(\hat{\mathbf{n}})\right], \qquad \Theta(\hat{\mathbf{n}}) \equiv \frac{\Delta T(\hat{\mathbf{n}})}{\bar{T}}. \tag{1}$$

The anisotropies are small,

$$\Theta \sim 10^{-5}, \tag{2}$$

but they encode the primordial perturbations, the composition of the plasma, and the geometry between recombination and today.

Key idea

The CMB is not merely a thermal relic. It is a projected image of primordial curvature perturbations processed by the photon–baryon plasma.

From primordial perturbations to observables

The central object describing the initial conditions is the comoving curvature perturbation $\mathcal{R}(\mathbf{k})$. For adiabatic perturbations it is conserved on super-horizon scales, so it can be used to connect the early Universe to the CMB and large-scale structure.

The logical chain is

$$\mathcal{R}(\mathbf{k}) \quad \longrightarrow \quad \Theta(\hat{\mathbf{n}}) \quad \longrightarrow \quad C_\ell \quad \longrightarrow \quad P_m(k, z). \tag{3}$$

In linear theory this chain is calculable. The primordial random field supplies the initial conditions, while transfer functions describe the subsequent evolution through radiation, matter, and dark-energy domination.

Physical message

CMB anisotropies and large-scale structure are two late-time images of the same primordial curvature perturbations.

Linear cosmological perturbations

To describe structure formation, one expands around the homogeneous FLRW background. For the density field,

$$\rho(\mathbf{x}, t) = \bar{\rho}(t) + \delta\rho(\mathbf{x}, t), \qquad \delta(\mathbf{x}, t) \equiv \frac{\delta\rho(\mathbf{x}, t)}{\bar{\rho}(t)}. \tag{4}$$

The metric is also perturbed,

$$g_{\mu\nu} = \bar{g}_{\mu\nu} + h_{\mu\nu}, \qquad |h_{\mu\nu}| \ll 1. \tag{5}$$

At linear order, only first powers of the perturbations are retained. This makes the evolution equations linear, and different Fourier modes evolve independently.

Newtonian gauge

For scalar perturbations, a useful representation is the Newtonian gauge,

$$\mathrm{d}s^2 = -(1+2\Phi)\mathrm{d}t^2 + a^2(t)(1-2\Psi)\mathrm{d}\mathbf{x}^2. \tag{6}$$

The potentials Φ and Ψ describe the scalar perturbations of the spacetime geometry. In the absence of anisotropic stress,

$$\Phi = \Psi. \tag{7}$$

Perturbation variables depend on the choice of time slicing. The gauge-invariant curvature perturbation $\mathcal{R}$ is especially useful because, for adiabatic perturbations, it becomes conserved on scales larger than the Hubble radius.

Fourier decomposition

Perturbations are decomposed into Fourier modes using the convention

$$\delta(\mathbf{x}, t) = \int \frac{\mathrm{d}^3\mathbf{k}}{(2\pi)^3} \delta(\mathbf{k}, t) e^{i\mathbf{k}\cdot\mathbf{x}}. \tag{8}$$

A mode with comoving wavenumber $k = |\mathbf{k}|$ corresponds to a comoving wavelength

$$\lambda = \frac{2\pi}{k}. \tag{9}$$

The comparison with the comoving Hubble radius organizes the physics. A mode is outside the Hubble radius when $k \ll aH$, and it re-enters when

$$k = aH. \tag{10}$$

Key simplification

In linear theory, one solves the evolution of each Fourier mode independently and then reconstructs the statistical field.

Power spectrum convention

Primordial perturbations are stochastic, so their information is encoded statistically. With the Fourier convention above, statistical homogeneity and isotropy imply

$$\langle \delta(\mathbf{k})\delta^*(\mathbf{k}')\rangle = (2\pi)^3\delta^{(3)}(\mathbf{k}-\mathbf{k}')P_\delta(k). \tag{11}$$

The dimensionless spectrum is defined as

$$\mathcal{P}_\delta(k) \equiv \frac{k^3}{2\pi^2}P_\delta(k), \tag{12}$$

so that the variance is

$$\langle \delta^2\rangle = \int \mathcal{P}_\delta(k)\,\mathrm{d}\ln k. \tag{13}$$

Interpretation

$P_\delta(k)$ carries dimensions, while $\mathcal{P}_\delta(k)$ gives the contribution to the variance per logarithmic interval in wavenumber.

Primordial curvature perturbation

The primordial initial conditions are most conveniently described by the curvature perturbation $\mathcal{R}$. In the Newtonian-gauge convention used here, on comoving hypersurfaces one may write

$$\mathcal{R} = -\Psi, \tag{14}$$

up to sign conventions for the scalar metric perturbation.

For adiabatic perturbations,

$$\mathcal{R}_k \simeq \text{constant} \qquad \text{for} \qquad k \ll aH. \tag{15}$$

The primordial curvature spectrum is defined by

$$\langle \mathcal{R}(\mathbf{k})\mathcal{R}^*(\mathbf{k}')\rangle = (2\pi)^3 \delta^{(3)}(\mathbf{k} - \mathbf{k}') P_{\mathcal{R}}(k), \tag{16}$$

with

$$\mathcal{P}_{\mathcal{R}}(k) \equiv \frac{k^3}{2\pi^2} P_{\mathcal{R}}(k). \tag{17}$$

Primordial spectrum

The simplest inflationary initial conditions are described by an approximately power-law curvature spectrum,

$$\mathcal{P}_{\mathcal{R}}(k) = A_s \left(\frac{k}{k_*}\right)^{n_s - 1} . \tag{18}$$

Exact scale invariance corresponds to $n_s = 1$. Observations find a slightly red spectrum,

$$n_s \simeq 0.965, \tag{19}$$

so that the amplitude is slightly larger on large scales than on small scales.

The observed CMB is consistent with perturbations that are nearly Gaussian, nearly scale invariant, and predominantly adiabatic. These properties are naturally produced by simple single-clock inflationary models.

Adiabatic perturbations

Adiabatic perturbations correspond to fluctuations that can be interpreted as local time shifts of the homogeneous background evolution.

Equivalently, all particle species share the same perturbation along their equilibrium trajectory,

$$\frac{\delta n_i}{\dot{\bar{n}}_i} = \frac{\delta n_j}{\dot{\bar{n}}_j} \equiv \delta t(\mathbf{x})\,. \tag{20}$$

For photons, baryons, and cold dark matter this gives

$$\delta_\gamma = \frac{4}{3}\delta_b = \frac{4}{3}\delta_c. \tag{21}$$

In this case all components are overdense or underdense in the same regions, with no change in the relative composition of the plasma.

Isocurvature perturbations

Isocurvature perturbations correspond instead to fluctuations in the relative composition of the plasma at fixed total energy density.

They are described by entropy perturbations,

$$S_{ij} = \frac{\delta n_i}{n_i} - \frac{\delta n_j}{n_j}. \tag{22}$$

On super-horizon scales, a pure isocurvature mode initially satisfies

$$\delta\rho_{\rm tot} = 0, \qquad \mathcal{R}_{\rm ini} = 0. \tag{23}$$

The total energy density is initially unperturbed, but different species fluctuate out of phase. Such perturbations can arise from additional light fields, for example axion-like degrees of freedom, and are strongly constrained by the CMB.

Transfer functions

The connection between primordial curvature perturbations and late-time observables is linear at first order. Schematically,

$$\delta_i(k,\eta) = T_i(k,\eta)\mathcal{R}(k), \qquad (24)$$

where T_i is a transfer function determined by the Einstein–Boltzmann equations.

For the CMB temperature anisotropy,

$$\Theta(\hat{\mathbf{n}}) = \int \frac{\mathrm{d}^3 k}{(2\pi)^3}\mathcal{R}(\mathbf{k})\Delta_T(k, \hat{\mathbf{k}}\cdot\hat{\mathbf{n}}). \qquad (25)$$

The transfer function contains gravitational redshift, acoustic oscillations, Doppler effects, diffusion damping, and the projection from three-dimensional Fourier modes to the two-dimensional sky.

Large-angle limit: Sachs–Wolfe effect

On angular scales much larger than the sound horizon at recombination, the dominant contribution is the ordinary Sachs–Wolfe effect,

$$\Theta(\hat{\mathbf{n}}) \simeq \left(\frac{1}{4}\delta_\gamma + \Phi \right)_{\eta_*} . \tag{26}$$

During matter domination, for adiabatic perturbations,

$$\Theta(\hat{\mathbf{n}}) \simeq \frac{1}{3}\Phi(\eta_*, \mathbf{x}_*). \tag{27}$$

Using the matter-era relation

$$\Phi = -\frac{3}{5}\mathcal{R}, \tag{28}$$

one obtains

$$\Theta \simeq -\frac{1}{5}\mathcal{R}. \tag{29}$$

This explains why large-angle CMB anisotropies directly probe the primordial curvature perturbation.

Spherical harmonic decomposition

The observed temperature field on the sky is expanded in spherical harmonics,

$$\Theta(\hat{\mathbf{n}}) = \sum_{\ell=0}^{\infty} \sum_{m=-\ell}^{\ell} a_{\ell m} Y_{\ell m}(\hat{\mathbf{n}}). \tag{30}$$

Statistical isotropy implies

$$\langle a_{\ell m} a^*_{\ell' m'} \rangle = C_\ell \delta_{\ell\ell'} \delta_{mm'}. \tag{31}$$

For one observed sky, the angular power spectrum is estimated as

$$C_\ell = \frac{1}{2\ell+1} \sum_{m=-\ell}^{\ell} |a_{\ell m}|^2. \tag{32}$$

From $\mathcal{P}_{\mathcal{R}}(k)$ to C_ℓ

In linear theory the CMB angular spectrum is obtained by convolving the primordial curvature spectrum with radiation transfer functions:

$$C_\ell^{TT} = 4\pi \int \frac{\mathrm{d}k}{k} \mathcal{P}_{\mathcal{R}}(k) \left[\Delta_\ell^T(k)\right]^2 . \qquad (33)$$

Here $\Delta_\ell^T(k)$ contains all late-time linear physics from horizon re-entry to observation.

Separation of physics

$$\boxed{\text{initial conditions: } \mathcal{P}_{\mathcal{R}}(k)} \quad \times \quad \boxed{\text{plasma, gravity, projection: } \Delta_\ell^T(k)} . \qquad (34)$$

Tight coupling before recombination

Before recombination, photons scatter rapidly off free electrons through Thomson scattering, while electrons remain electromagnetically coupled to baryons. The photon–baryon system therefore behaves approximately as a single fluid.

The tight-coupling condition is

$$\Gamma_\gamma = n_e \sigma_T c \gg H. \tag{35}$$

Radiation pressure supplies the restoring force, while baryons contribute inertia. This competition between pressure and gravity is the origin of acoustic oscillations in the pre-recombination plasma.

Photon–baryon acoustic oscillator

For a Fourier mode in conformal time, the photon density perturbation obeys schematically

$$\delta_\gamma'' + c_s^2 k^2 \delta_\gamma \simeq \text{gravitational driving.} \tag{36}$$

The sound speed of the photon–baryon fluid is

$$c_s^2 = \frac{1}{3(1+R_b)}, \qquad R_b \equiv \frac{3\rho_b}{4\rho_\gamma}. \tag{37}$$

The factor R_b measures baryon loading. Baryons increase the inertia of the coupled fluid without contributing appreciable pressure, thereby reducing the sound speed relative to the pure-radiation value $c_s^2 = 1/3$.

Sound horizon

If the gravitational potential varies slowly, the acoustic solution is approximately oscillatory,

$$\delta_\gamma(k,\eta) \simeq A(k)\cos[kr_s(\eta)] + B(k)\sin[kr_s(\eta)]\,. \tag{38}$$

The comoving sound horizon is

$$r_s(\eta) = \int_0^\eta c_s(\eta')\,\mathrm{d}\eta'. \tag{39}$$

It is the maximum comoving distance that an acoustic wave can propagate before a given time. At recombination, it is approximately

$$r_s(\eta_*) \simeq 150\,\mathrm{Mpc}. \tag{40}$$

At recombination, the Thomson scattering rate drops below the Hubble rate,

$$\Gamma_\gamma = n_e \sigma_T c \simeq H. \tag{41}$$

The photon mean free path grows rapidly, photons decouple from baryons, and the acoustic pattern is projected onto the sky.

Modes caught at extrema of their acoustic oscillation generate peaks. The approximate peak condition is

$$k_m r_s(\eta_*) \simeq m\pi, \qquad m = 1, 2, 3, \dots. \tag{42}$$

Projection to angular multipoles gives

$$\ell_m \simeq k_m D_A(\eta_*) \simeq m\pi \frac{D_A(\eta_*)}{r_s(\eta_*)}. \tag{43}$$

The first acoustic peak occurs at approximately $\ell \sim 200$.

Physical interpretation of the acoustic peaks

The peak positions are controlled mainly by the angular size of the sound horizon,

$$\theta_* \equiv \frac{r_s(\eta_*)}{D_A(\eta_*)}. \tag{44}$$

The peak heights encode the composition of the pre-recombination plasma. Baryons increase the inertia of the photon–baryon fluid and enhance compressional peaks. Dark matter controls the time evolution of gravitational potentials. Radiation changes the expansion rate before recombination, and photon diffusion suppresses anisotropies at small angular scales.

CMB as a parameter machine

The detailed pattern of peaks converts early-Universe microphysics into precision measurements of Ω_b, Ω_c, H_0, n_s, A_s, and related cosmological parameters.

Silk damping

Tight coupling is not exact. Before recombination, photons have a finite mean free path and therefore diffuse through the plasma. This diffusion erases perturbations below a characteristic damping scale.

The transfer function acquires an approximate exponential suppression,

$$\Delta_\ell^T(k) \longrightarrow \Delta_\ell^T(k) \exp\left[-\frac{k^2}{k_D^2}\right]. \tag{45}$$

The damping scale is controlled by the photon mean free path and the expansion rate. Physically, photons random-walk out of overdense regions and smooth temperature contrasts.

The damping tail

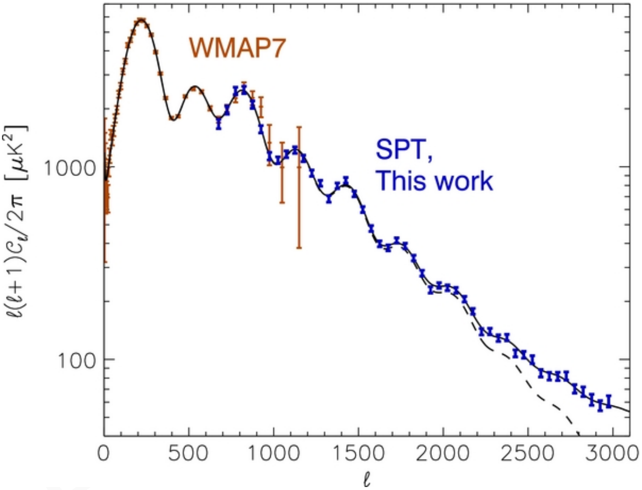

Figure: CMB temperature power spectrum showing acoustic peaks and the damping tail at large multipoles, caused by photon diffusion before recombination.

From the CMB to structure formation

The CMB provides a snapshot of perturbations at recombination. After recombination, photons free-stream while matter perturbations continue to evolve gravitationally.

On large scales the evolution remains linear for a long time. On small scales, gravitational collapse eventually becomes nonlinear and produces galaxies, clusters, and the cosmic web.

Core question

How does the primordial curvature spectrum $\mathcal{P}_{\mathcal{R}}(k)$ become the late-time matter power spectrum $P_m(k, z)$?

Growth equation for matter perturbations

On sub-horizon scales, pressureless matter perturbations can be treated using Newtonian equations in an expanding background. Combining the continuity, Euler, and Poisson equations gives

$$\ddot{\delta}_m + 2H\dot{\delta}_m - 4\pi G\bar{\rho}_m\delta_m = 0. \tag{46}$$

The gravitational term amplifies overdensities, while the term $2H\dot{\delta}_m$ acts as Hubble friction.

During matter domination, the growing solution is

$$\delta_m \propto a. \tag{47}$$

During radiation domination the growth of matter perturbations is strongly suppressed, while during dark-energy domination accelerated expansion slows the growth.

Linear growth factor

In the linear regime the time dependence of matter perturbations is described by the growth factor $D(a)$,

$$\delta_m(\mathbf{k}, a) = D(a)\delta_m(\mathbf{k}, a_i). \tag{48}$$

The growth factor obeys

$$\ddot{D} + 2H\dot{D} - 4\pi G\bar{\rho}_m D = 0. \tag{49}$$

For scale-independent linear growth,

$$P_m(k, a) \propto D^2(a). \tag{50}$$

Matter power spectrum

The large-scale distribution of matter is described statistically by the matter power spectrum,

$$\langle \delta_m(\mathbf{k}, a)\delta_m^*(\mathbf{k}', a)\rangle = (2\pi)^3\delta^{(3)}(\mathbf{k} - \mathbf{k}')P_m(k, a). \tag{51}$$

The dimensionless matter spectrum is

$$\mathcal{P}_m(k, a) = \frac{k^3}{2\pi^2}P_m(k, a). \tag{52}$$

Large k corresponds to small physical scales, while small k corresponds to large scales.

From primordial curvature to matter clustering

The observed matter power spectrum is not primordial. It is the evolved form of the initial curvature perturbations.

A useful schematic relation is

$$P_m(k,z) = \frac{2\pi^2}{k^3}\,\mathcal{P}_{\mathcal{R}}(k)\left[\frac{2k^2}{5\Omega_m H_0^2}\,T_m(k)D(z)\right]^2. \qquad (53)$$

Here $T_m(k)$ is the matter transfer function and $D(z)$ is the late-time growth factor. The transfer function encodes the scale-dependent evolution before ordinary matter-era growth.

Physical meaning

Different modes evolve differently because they enter the Hubble radius at different epochs.

Equality scale and transfer suppression

The characteristic scale in the matter transfer function is set by the horizon size at matter–radiation equality,

$$k_{\rm eq} \sim a_{\rm eq} H_{\rm eq}. \tag{54}$$

Modes with $k \ll k_{\rm eq}$ enter the Hubble radius after equality and are not strongly suppressed. Modes with $k \gg k_{\rm eq}$ enter during radiation domination, when matter is subdominant and grows only slowly.

This produces the turnover in the matter power spectrum near $k \sim k_{\rm eq}$, followed by suppressed small-scale power.

The BBKS transfer function

A useful analytic fit for the cold dark matter transfer function was given by Bardeen, Bond, Kaiser and Szalay. In the no-baryon approximation,

$$T_{\mathrm{BBKS}}(q) = \frac{\ln(1+2.34q)}{2.34q}\left[1+3.89q+(16.1q)^2+(5.46q)^3+(6.71q)^4\right]^{-1/4} \quad (55)$$

The variable q is conventionally written as

$$q \equiv \frac{k}{\Gamma h\,\mathrm{Mpc}^{-1}}, \qquad \Gamma \simeq \Omega_m h, \quad (56)$$

where Γ is the shape parameter.

BBKS captures the broad suppression of small-scale matter perturbations caused by horizon entry during radiation domination.

Shape of the matter power spectrum

The linear matter power spectrum may be written schematically as

$$P_m(k,z) = A\,k^{n_s}\,T_m^2(k)D^2(z). \tag{57}$$

On large scales, $T_m(k) \simeq 1$, so the spectrum follows the primordial slope. Around equality, the spectrum turns over. On small scales, modes entered during radiation domination and their growth was delayed until matter domination.

The turnover scale therefore measures the horizon size at matter–radiation equality, while the detailed small-scale shape is sensitive to baryons, neutrinos, dark matter, and the expansion history.

Numerical transfer functions

The BBKS formula is pedagogically useful, but precision cosmology requires solving the coupled Einstein–Boltzmann system. Modern calculations use numerical codes such as CAMB or CLASS.

These codes include baryon acoustic oscillations, recombination physics, neutrino effects, photon diffusion, lensing, and dark-energy evolution.

Pedagogical role of analytic fits

Analytic transfer functions explain the origin of the turnover and the suppression of small-scale power. Numerical transfer functions provide the precision required for comparison with observations.

Matter power spectrum: observations

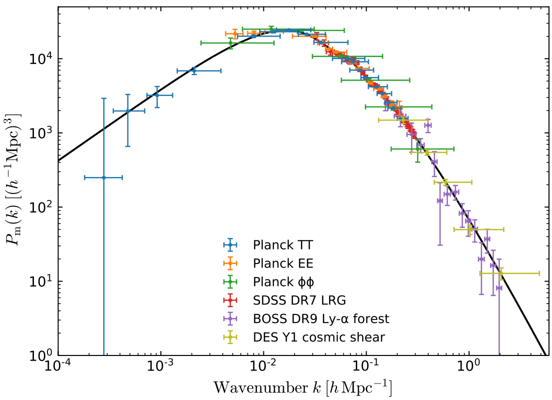

Figure: Measurements of the linear matter power spectrum from CMB, galaxy surveys, Lyman-α forest, and weak lensing probes.

Transfer function: analytical vs numerical

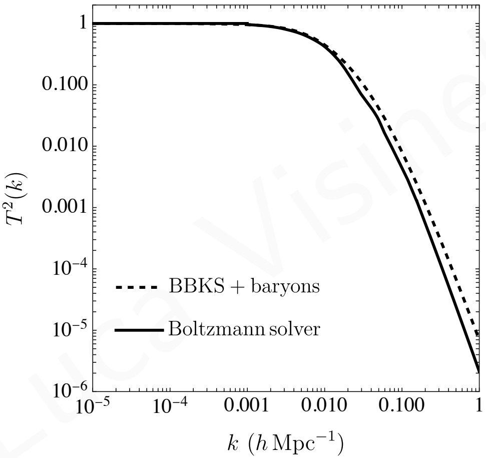

Figure: Comparison between an analytic fitting formula and the full linear-theory transfer function.

BAO as the late-time relic of sound waves

Before recombination, baryons participate in the same acoustic oscillations that generate the CMB peaks. After recombination, photons decouple and free-stream, while baryons fall into the gravitational potentials dominated by dark matter.

The sound horizon scale remains imprinted in the late-time matter distribution:

$$r_s(\eta_*) = \int_0^{\eta_*} c_s(\eta)\,\mathrm{d}\eta \sim 150\,\mathrm{Mpc}. \tag{58}$$

Thus the same physical scale appears both as the acoustic scale in the CMB and as a preferred separation in galaxy clustering.

In real space, the acoustic scale appears as an enhanced probability of finding pairs of galaxies separated by approximately the sound horizon.

In Fourier space, the same effect appears as small oscillatory features in the matter power spectrum,

$$P_m(k) = P_{\rm smooth}(k)\left[1 + O_{\rm BAO}(k)\right]. \tag{59}$$

BAO are therefore the late-time fossil of sound waves in the pre-recombination photon–baryon plasma.

BAO as a standard ruler

The sound horizon is calculable from early-Universe physics and provides a robust comoving standard ruler.

Transverse BAO measurements constrain the angular diameter distance $D_A(z)$, while radial BAO measurements constrain the Hubble rate $H(z)$. Together they provide a powerful probe of the late-time expansion history.

Key point

BAO connect early-Universe plasma physics to late-time cosmic geometry.

Matter power spectrum with BAO

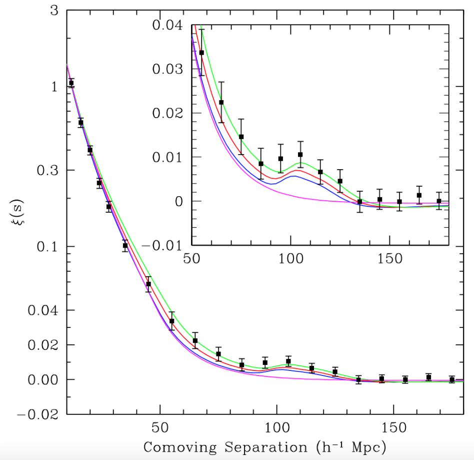

Figure: Matter power spectrum showing baryon acoustic oscillation wiggles from sound waves in the pre-recombination photon–baryon plasma.

One physical story

The CMB and large-scale structure are connected by a single sequence of physical processes.

Primordial curvature perturbations $\mathcal{R}$ provide the initial conditions. Before recombination, photon–baryon perturbations oscillate acoustically. Recombination freezes the photon pattern and projects it onto the sky as CMB acoustic peaks. After recombination, matter perturbations continue to grow gravitationally. Horizon entry and radiation-era suppression shape the matter transfer function, while the same sound horizon appears later as BAO in galaxy clustering.

Core synthesis

CMB anisotropies and large-scale structure are complementary probes of the same primordial perturbations, processed by different transfer functions.

Summary

Primordial curvature perturbations provide the initial conditions for both CMB anisotropies and large-scale structure. The CMB temperature spectrum follows from

$$C_\ell^{TT} = 4\pi \int \frac{\mathrm{d}k}{k} \mathcal{P}_\mathcal{R}(k) \left[\Delta_\ell^T(k)\right]^2 . \tag{60}$$

Acoustic oscillations arise from the competition between gravity and radiation pressure in the photon–baryon fluid. The sound horizon sets both the CMB acoustic scale and the BAO standard ruler.

The matter power spectrum is shaped by the primordial spectrum, radiation-era transfer suppression, BAO wiggles, and late-time growth. Together, CMB and LSS observations provide precision tests of the ΛCDM model.